Ultra-low thermal conductivity in scheelite and A-deficient scheelite ceramics

Eliane Bsaibess, Fabian Delorme, Isabelle Monot-Laffez, Fabien Giovannelli

Version of Record: https://www.sciencedirect.com/science/article/pii/S135964622100230X
Manuscript_78f7e078c128d5407305bb96d8c2471b

Ultra-low thermal conductivity in scheelite and A-deficient scheelite ceramics

Eliane Bsaibess, Fabian Delorme, Isabelle Monot-Laffez, and Fabien Giovannelli

Universite de Tours, CNRS, INSA CVL, GREMAN UMR 7347, IUT de Blois 15 rue de la chocolaterie, 41029 Blois Cedex, France

April 19, 2021

Abstract

Synthesis of scheelite-type oxides based on lanthanum and barium molybdate ($BaMoO_4$ and $La_2Mo_3O_{12}$ ceramics) were successfully prepared via conventional solid-state reaction method. Dense ceramics were obtained by conventional sintering. Structural, microstructural and thermal properties of both sintered ceramics were assessed to identify the impact of cation deficiency on thermal conductivity. $BaMoO_4$ ceramic has shown a decrease in thermal conductivity from $0.8\,W\,m^{-1}\,K^{-1}$ to $0.65\,W\,m^{-1}\,K^{-1}$ from 400 K to 650 K. The deficient scheelite $La_2Mo_3O_{12}$ compound was found to further reduce thermal conductivity. An ultra-low thermal conductivity constant value of about $0.59\text{-}0.62\,W\,m^{-1}\,K^{-1}$ was calculated over the entire temperature range. This value is the lowest recorded value for oxides so far discovered and such materials may be promising ones for thermal insulating applications.

Materials exhibiting a low thermal conductivity are the key components in several areas such as thermal barrier coatings (TBCs) or thermoelectric materials. TBCs have been the subject of considerable research over the past few decades, driven by the demands for improved efficiency and substantially higher operating temperatures required for future gas turbine applications [1–3]. To date, extensive efforts have been dedicated to explore insulator materials with low thermal conductivity. Considering its high temperature stability and low thermal conductivity (below $3\,W\,m^{-1}\,K^{-1}$ [4], the (6–8)wt% yttria stabilized zirconia (YSZ) [5, 6] has been widely used as bond and top coat for thermal barrier coatings systems. With continuous improvements, several TBCs materials have been proposed to replace YSZ, such as rare earth zirconates [7, 8], pyrochlore oxides [9], magnetoplumbite [10, 11], perovskite [12], garnet [13] and metal phosphate [14]. Such materials have been extensively investigated showing a low thermal conductivity ranging from 1.2 to $2\,W\,m^{-1}\,K^{-1}$ in the temperature range from 25 °C to 700 °C. Moreover, several studies have revealed the potential of lanthanum molybdate ($La_2Mo_2O_9$) as promising candidates for TBC material having lower thermal conductivity ($0.95\,W\,m^{-1}\,K^{-1}$ at 1273 K) than the current TBC materials [4, 15–18]. As Winter and Clarke pointed out, the low thermal conductivity may be attributed to the presence of several cation sublattices, large mean atomic mass and high concentration of structural oxygen vacancies [4]. For thermoelectric applications, an efficient material should exhibit high power factor and low thermal conductivity. Therefore, tremendous efforts have been made to reduce thermal conductivity of semiconductors by nanostructuring, composite and defect chemistry approaches [19–23]. However, for high temperature applications, stability of nanostructures may be an issue [23], and the thermoelectric community is actively looking for new materials with low intrinsic thermal conductivity [24–31]. Recently, Liu et al. have predicted very low thermal conductivity of scheelite type structure [32]. Scheelite oxides with general formula ABO_4 consists of strong units of BO_4 tetrahedra, week units of AO_8 as well as the anisotropy in A-O and B-O bonds that allow them having low thermal conductivity and mechanical properties which eventually can fulfil the requirements for next generation TBC materials. Various molybdenum- and tungsten-based scheelites (Ca, Sr, Ba) (Mo, W) O4 have been reported, by Liu et al. [32], predicting good intrinsic quasi-ductility and ultra-low thermal conductivity , ranging in 0.556 - $1.2\,W\,m^{-1}\,K^{-1}$ which is lower than common thermal

insulating materials such as YSZ and pyrochlore oxides. Interestingly, in this study, results from previous experimental evidence and simulations models are successfully conducted. It is found that experimental result of thermal conductivity of $BaWO_4$ ($1.63\,W\,m^{-1}\,K^{-1}$ at 563 K) is consistent with theoretical predictions of Debye-Callaway model, thereby offering promising potential in exploring such materials for TBC applications. Among the compositions studied by Liu et al. [32], $BaMoO_4$ thermal conductivity is expected to reach value below $1\,W\,m^{-1}\,K^{-1}$ according to the Debye-Callaway model. Another approach applied for reducing thermal conductivity consists in introducing defects on the cationic sublattice. Several studies reported that A-site deficiency in perovskite structures yields to lower thermal conductivity values [33, 34]. Furthermore, Brixner et al. [35] have previously evidenced that it is easy to bring high defect concentrations at the A site of scheelites, and shown that vacancies can be as high as 1/3 in some rare-earth molybdate systems such as $La_{0.67}\square_{0.33}MoO_4$ (also written as $La_2Mo_3O_{12}$) where $\square$ stands for the vacancy site [35]. Assuming that such model predictions and experimental investigations are potentially valuable for improving TBC materials, our contribution in this work consists in studying structural and thermal properties of barium molybdate ($BaMoO_4$) belonging to scheelite family and the defect scheelite-type structure $La_2Mo_3O_{12}$. Both ceramics were elaborated by solid state reaction method. A systematic study of the thermal conductivity of both samples was investigated from room temperature to 1000 K and differences were discussed.

$BaMoO_4$ and $La_2Mo_3O_{12}$ ceramic samples were fabricated by conventional solid-state reaction starting from a stoichiometric mixture of the corresponding component oxides: $BaCO_3$ (99.9%), MoO_3 (99.9%) and La_2O_3 (99.9%), purchased from ChemPur company. MoO_3 and La_2O_3 reactants were preheated before weighing in air atmosphere respectively at 300 °C and 1000 °C overnight. The precursors were then grounded in planetary ball mill of tungsten carbide for 5 minutes at 300 rpm (Retsch PM 100). The mixed powders were then calcined in an alumina crucible, in a muffle furnace at 850 °C for 8 h at a heating rate of $5\,°C\,min^{-1}$ in air, to ensure the single-phase formation. The calcined powders were then reground with few drops of polyvinyl alcohol (PVA) solution (2 wt% in water) and cold-pressed into pellets of about 13 mm in diameter. Finally, $BaMoO_4$ and $La_2Mo_3O_{12}$ pellets were heated in an alumina crucible at a heating rate of $5\,°C\,min^{-1}$, up to 650 °C for 2 h to drive off the PVA and then sintered respectively at 1100 °C and 980 °C for 4 h each. The density was determined from the weight and the calculated volume of the pellets.

The presence of tetragonal scheelite crystal structure and its phase purity were confirmed by X-ray diffraction (XRD) measurements [Bruker D8 advance diffractometer with CuKα radiations λ 1.5418 Å]. XRD patterns were collected with a scanning speed of 2.4° (2Θ)/min with a step size of 0.02° over an angular range from 20° to 80° at room temperature. The microstructures of the samples were examined using scanning electron microscopy (TESCAN – MIRA 3 SEM) operating in backscattered electron (BSE) emission mode. The elementary composition was also analysed by Energy Dispersive X-ray (EDX) coupled to SEM with an acceleration voltage of 20 kV and a current of 20 pA. For both samples, a gold coating was deposited in order to reveal the surface and provide a conductive path for electrons.

The laser flash method (Netzsch LFA 457 instrument) was adopted for the measurement of the thermal diffusivity. Samples were coated with a thin layer of graphite in order to improve absorption of the laser light and then fixed in the holders of the LFA apparatus (6 × 6 mm). The measurements were carried out from 400 to 1000 K at 100 K intervals in a primary vacuum after three N_2 purges. In order to guarantee the reliability of the testing data, thermal diffusivity value was recorded three times at each temperature for averaging.

Specific heat capacity of both samples was evaluated by Differential Scanning Calorimeter (DSC, Netzsch STA 449 F3 Jupiter) analysis. The powdered samples of about 50 mg were spread evenly in a platinum crucible and heated continuously up to 1000 K under nitrogen atmosphere with a heating rate of $20\,K\,min^{-1}$. In conjunction with the DSC analysis, a Netzsch dilatometer (402 CL) was used to measure the thermal expansion evolution of the sintered $La_2Mo_3O_{12}$ pellet as a function of the temperature. Measurements were conducted during a single heating cycle from 400 to 1100 K at a heating rate of $10\,K\,min^{-1}$.

Based on the obtained experimental data of the thermal diffusivity (D), the heat capacity (C_p), and the

density (ρ), one can deduce the thermal conductivity coefficient (κ) of both samples as follows:

$$\kappa = D \times C_p \times \rho \tag{1}$$

The as-sintered pellets were white in colour. The theoretical density of pure $BaMoO_4$ and $La_2Mo_3O_{12}$ is 4.738 and 4.865 g cm^{-3}, respectively [36, 37]. The maximum achieved relative density is $\approx$ 95% and $\approx$ 92% of theoretical value for $BaMoO_4$ and $La_2Mo_3O_{12}$ after sintering at 1100 °C and 980 °C for 4 h each, respectively.

X-ray diffraction patterns of both $BaMoO_4$ and $La_2Mo_3O_{12}$ ceramics sintered are shown in figure 1. One can notice that both $BaMoO_4$ and $La_2Mo_3O_{12}$ exhibited strong and well-defined XRD peaks indicating crystallinity of both compounds. All diffraction peaks of $BaMoO_4$, at room temperature, are clearly matching the scheelite-type tetragonal structure with $I4_1/a$ space group and indexed according to the standard data of tetragonal $BaMoO_4$ (JCPDS No.29-0193) [36]. For $La_2Mo_3O_{12}$ compound, the structure is more complex because of the presence of vacancies. The main diffraction peaks can be indexed by the monoclinic phase with C_2/a space group consistent with previous reports [37]. The remaining peaks observed may correspond to reflections of $La_2Mo_2O_9$ impurity.

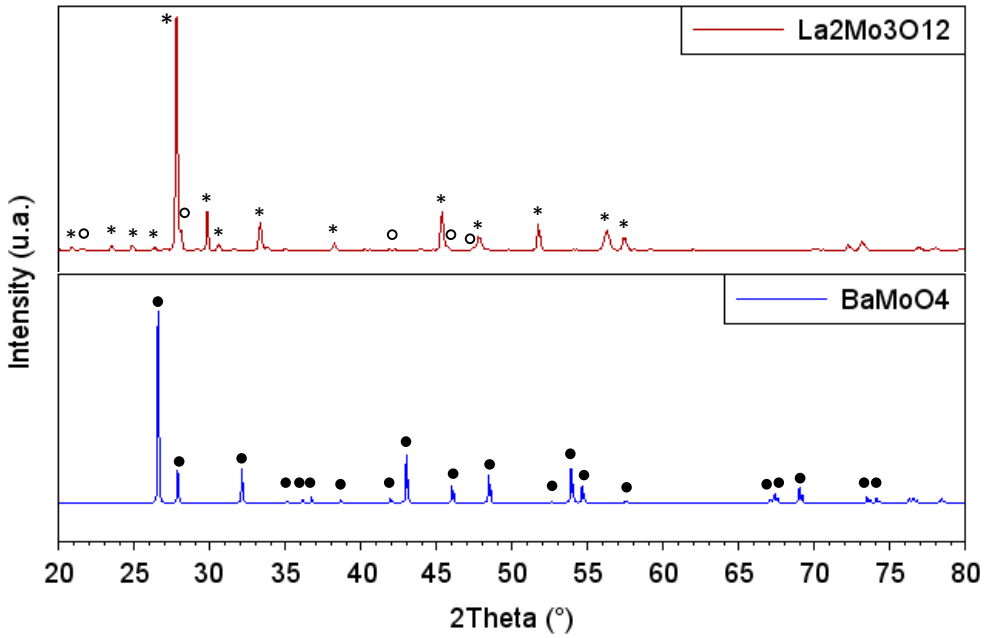

Figure 1: XRD patterns of the obtained $BaMoO_4$ and $La_2Mo_3O_{12}$ sintered ceramics at room temperature: (*) monoclinic $La_2Mo_3O_{12}$, (○) $La_2Mo_2O_9$ and (●) tetragonal $BaMoO_4$

The scanning electron microscopic study of both fractured surfaces of $BaMoO_4$ and $La_2Mo_3O_{12}$ sintered ceramics are shown in figure 2. It is observed from the micrographs a dense and fine microstructure. The grain sizes are estimated from SEM micrographs. For both samples, the SEM images exhibit grain size ranging from 7 to 15 µm. The average grain size is circa 11 µm and 9 µm for $BaMoO_4$ and $La_2Mo_3O_{12}$, respectively. Some voids and pores can be observed for $La_2Mo_3O_{12}$ and $BaMoO_4$ ceramics, which is consistent with the relative density of about 92% and 95% respectively. EDX analyses or backscattered electrons images were unable to identify $La_2Mo_2O_9$ impurity.

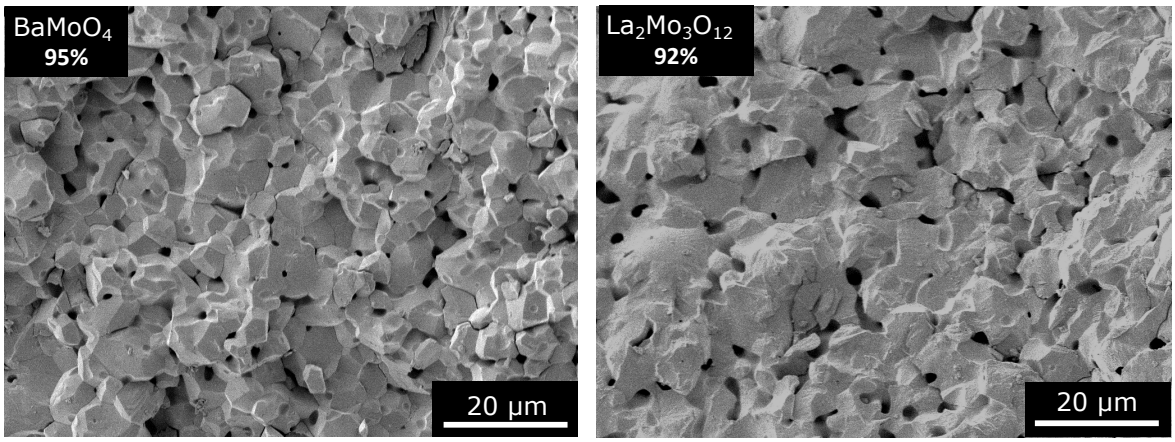

Figure 2: BSE-SEM micrograph of the fractured surfaces of $BaMoO_4$ and $La_2Mo_3O_{12}$ sintered ceramics

The measured heat capacities of $BaMoO_4$ and $La_2Mo_3O_{12}$ in the temperature range of 400 K to 1000 K are shown in figure 3. For $BaMoO_4$, our data are consistent with the Calvet micro-calorimeter measurements of Singh et al. [38] and they also join smoothly and have similar evolution with measurements made by Saha et al. [39] and Kubaschewsi et al. [40]. For those studies, the reported heat capacity data varies from about $0.4\,J\,g^{-1}\,K^{-1}$ across 300 K to $0.7\,J\,g^{-1}\,K^{-1}$ at 1800 K. The heat capacity of $La_2Mo_3O_{12}$ have been measured for the first time. A peak at around 850 K can be observed. It indicates that material undergoes a reversible ferroelastic phase transition behavior from monoclinic ($P2_1/a$) phase at low temperatures to orthorhombic (Pnca) phase at high temperatures. Accordingly, Sleight et al. [41] have reported that $A_2(MoO_4)_3$ compounds with monoclinic crystal structure at room temperature show a transition between 25 and 600 °C. The small magnitude of the heat effect accompanying the phase transition in $A_2M_3O_{12}$ samples could be based on the rotation of polyhedral network of the lattice [42, 43].

As $La_2Mo_3O_{12}$ shows phase transition around 850 K, the dilatometric thermal expansion behavior was also analysed in order to evaluate the impact of phase transition on the dilatation during heat treatment up to 1100 K with a rate of $10\,K\,min^{-1}$. Results reveal that the as-sintered $La_2Mo_3O_{12}$ exhibits a positive thermal expansion coefficient. This latter is approximately linear and does not display discontinuities. Therefore, the phase transition from a monoclinic to an orthorhombic form is not reflected. The $La_2Mo_3O_{12}$ compound exhibited a thermal expansion coefficient (α_L) ranging from 10 to $9 \times 10^{-6}\,K^{-1}$ at temperatures from 400 to 1100 K, indicating that α_L remains almost constant all along the temperature range. This result is consistent with previous results obtained on $La_2Mo_3O_{12}$ indicating an average linear expansion coefficient of about $6.9 \times 10^{-6}\,K^{-1}$ at 1000 K [44]. Therefore, this phase transition does not hinder the possibility to use $La_2Mo_3O_{12}$ compound as a TBC.

Using the above-mentioned parameters, the thermal conductivity was calculated by mean of equation 1. The temperature dependence of the thermal conductivity (κ) of both $La_2Mo_3O_{12}$ and $BaMoO_4$ sintered ceramics is illustrated in figure 4. $BaMoO_4$ thermal conductivity decreases from $0.8\,W\,m^{-1}\,K^{-1}$ at 400 K with increasing temperature and reaches $0.65\,W\,m^{-1}\,K^{-1}$ at 650 K and then increases up to $1.15\,W\,m^{-1}\,K^{-1}$. The $La_2Mo_3O_{12}$ thermal conductivity is almost constant starting from $0.59\,W\,m^{-1}\,K^{-1}$ at 400 K to $0.62\,W\,m^{-1}\,K^{-1}$ at 1000 K. As for measurement uncertainty, the overall average value of the relative standard uncertainty on the thermal conductivity was estimated to be ±11% [45]. Furthermore, in an attempt to exclude the effect of porosity, thermal conductivity values were normalized to represent values for 100% dense materials (κ_{dense}) using Maxwell's relation [4] as follow:

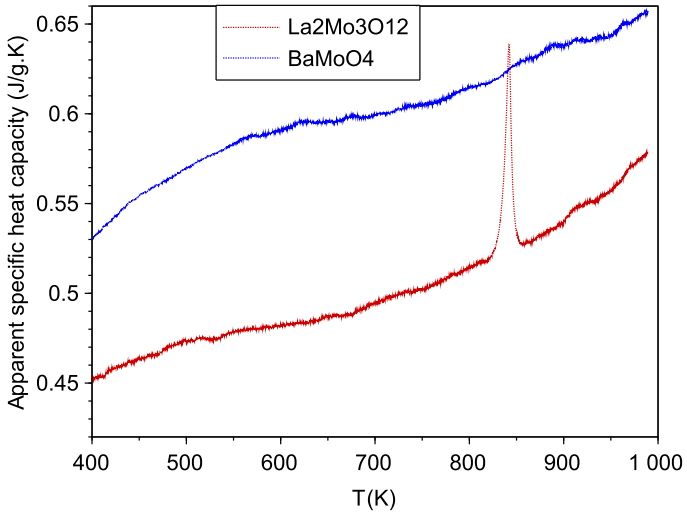

Figure 3: Mean heat capacity of $BaMoO_4$ and $La_2Mo_3O_{12}$ as function of temperature

$$\kappa_{dense} = \kappa_{measured} \times \frac{1}{1 - 1.5\Phi} \tag{2}$$

where Φ is the porosity.

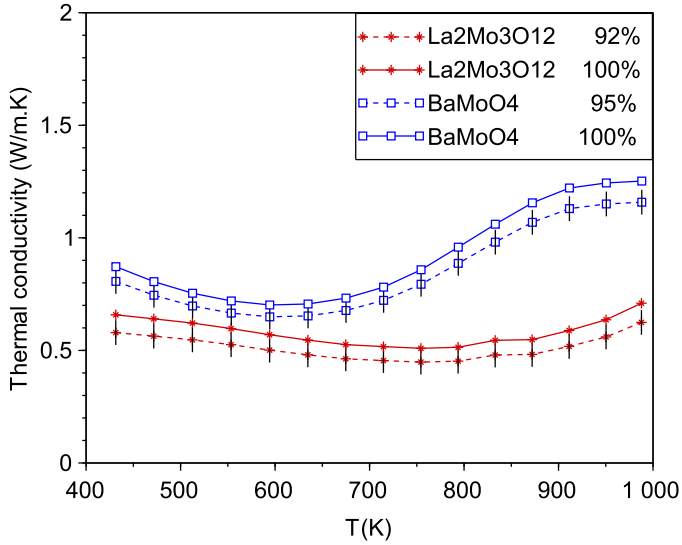

Figure 4: Calculated (solid line) and experimental (dash line) thermal conductivity of $La_2Mo_3O_{12}$ and $BaMoO_4$ sintered ceramics as a function of temperature. The vertical lines represents the total error bars.

The corrected data, obtained with 100% dense material show a thermal conductivity of 0.87 and

$0.65\,W\,m^{-1}\,K^{-1}$ at 400 K for $BaMoO_4$ and $La_2Mo_3O_{12}$, respectively.

As shown in figure 4, for $BaMoO_4$ sample, one can see that κ decreases from $\approx 0.87\,W\,m^{-1}\,K^{-1}$ at 400 K with increasing temperature and reaches $0.7\,W\,m^{-1}\,K^{-1}$ at 650 K. The values of κ are reasonably consistent with theoretical prediction based on Debye-Callaway model (κ^{1473}=$0.974\,W\,m^{-1}\,K^{-1}$) for the same composition [32], except for low temperature below 600 K. This discrepancy could originate from additional defects formed during the synthesis and sintering processes. As predicted, the $A^{+2}B^{+6}O_4$ scheelites structure possesses low thermal conductivity. The low thermal conductivity may be attributed to the structural feature of a BO_4 tetrahedron and the anisotropy in A - O and B - O bonds. However, thermal conductivity increases for temperatures higher than 700 K. This could be related to the enhanced radiative thermal conductivity. Indeed, the thermal diffusivity measured by laser flash method includes both the lattice and radiative contributions [46]. At low temperature, as the pellets were coated with carbon black as reported previously, radiation effect could be neglected and temperature dependence of thermal conductivity accords well with the 1/T law. However, at higher temperature as the carbon coating layer was gradually removed, and the pellet's color turns to white, the radiative effect arises indicating extensive internal optical scattering which was also reported in previous studies [4, 47].

In the case of $La_2Mo_3O_{12}$, the thermal conductivity value is almost constant starting from $0.65\,W\,m^{-1}\,K^{-1}$ at 400 K to $0.72\,W\,m^{-1}\,K^{-1}$ at 1000 K. Noticeably, in comparison to previous researches on $La_2Mo_2O_9$, for which the experimentally reported thermal conductivity varies from $0.82\,W\,m^{-1}\,K^{-1}$ at 400 K to $0.95\,W\,m^{-1}\,K^{-1}$ at 1000 K [4, 15, 17, 18], the A-deficiency of La in $La_2Mo_3O_{12}$ can significantly lower the thermal conductivity value as already reported for perovskite structure [33, 34]. As expected, by introducing vacancies on the scheelite structure an important decrease on thermal conductivity of about $\approx$ 23% compared to $BaMoO_4$ is obtained as a result of phonon scattering by point defects [33, 34, 47]. An ultra-low thermal conductivity of about 0.65 - $0.7\,W\,m^{-1}\,K^{-1}$ is obtained in the range of 400 - 1000 K. As far as the authors know, to date, this is the lowest thermal conductivity value reported for a dense crystalline oxide.

In conclusion, stoichiometric and cation deficient scheelite ceramic materials, $BaMoO_4$ and $La_2Mo_3O_{12}$ were prepared by a conventional solid-state route and sintered respectively at 1100 °C and 980 °C for 4 h in air. Dense ceramic bodies (95 and 92%, respectively) have been obtained. Structural and thermal properties of scheelite structures were studied. $BaMoO_4$ compound exhibited a low thermal conductivity, below $1\,W\,m^{-1}\,K^{-1}$ in the range 400-800 K. We reported an ultra-low thermal conductivity of $\approx$$0.65\,W\,m^{-1}\,K^{-1}$ for A-site deficiency $La_2Mo_3O_{12}$ compound, in the range of 400 - 1000 K. As far as the authors know, this is the lowest thermal conductivity value reported for a dense crystalline oxide. Therefore, scheelite-type structure provides a highly promising route to further improve thermal barrier coating materials. Relative to thermoelectric properties, low thermal conductivity is a first step, but electric transport properties should be improved by substitutions, doping or oxygen non-stoichiometry. This will be the subject of further studies.

Acknowledgements

The authors are grateful to Tatiana Chartier for technical support.

References

[1] D.R Clarke, M. Oechsner, N.P Padture, MRS Bull. 37 (2012) 891-898.

[2] N.P Padture, Nat. Mater. 15 (2016) 804-809.

[3] B. Liu, J. Wang, Y. Zhou, T. Liao, F. Li, Acta Mater. 55 (2007) 2949-2957.

[4] M.R. Winter, D.R. Clarke, J. Am. Ceram. Soc. 90 (2007) 533-540.

[5] J.G. Smeggil, Mater. Sci. Eng. 87 (1987) 261-265.

[6] Y. Bai, Z.H. Han, H.Q. Li, C. Xu, Y.L. Xu, C.H. Ding, J.F. Yang, Surf. Coat. Technol. 205 (2011) 3833-3839.

[7] J.R. Nicholls, K.J. Lawson, A. Johnstone, D.S. Rickerby, Surf. Coat. Technol. 151-152 (2002) 383-391.

[8] D. Zhu, R.A. Miller, Ceram. Eng. Sci. Proc. 23 (2002) 457-468.

[9] J.W. Fergus, Metall. Mater. Trans. E. 1 (2014) 118-131.

[10] X. Xie, H. Guo, S. Gong, H. Xu, J. Eur. Ceram. Soc. 31 (2011) 1677-1683.

[11] B. Jiang, M.H. Fang, Z.H. Huang, Y.G. Liu, P. Peng, J. Zhang, Mater. Res. Bull. 45 (2010) 1506-1508.

[12] M. Dietrich, R. Vaßen, D. Stöver, Ceramic Engineering and Science Proceedings. John Wiley & Sons, Inc. (2008) 637–643.

[13] N.P. Padture, P.G. Klemens, J. Am. Ceram. Soc. 80 (1997) 1018-1020.

[14] Y. Zhou, B. Liu, J. Eur. Ceram. Soc. 33 (2013) 2817-2821.

[15] E. Sabarthes, F. Delorme, V. Tezyk, C. Autret, G. Corbel, P. Lacorre, F. Giovannelli, Dalton Trans. 48 (2019) 10051-10061.

[16] X.Q. Cao, R. Vassen, D. Stoever, J. Eur. Ceram. Soc. 24 (2004) 1-10.

[17] H. Lu, C. A. Wang, J. Am. Ceram. Soc. 98 (2015) 1385-1388.

[18] K.M. Ok, Y. Ohishi, H. Muta, K. Kurosaki, S. Yamanaka, J. Eur. Ceram. Soc. 37 (2017) 281-288.

[19] B. Poudel, Q. Hao, Y. Ma, Y. Lan, A. Minnich, B. Yu, X. Yan, D. Wang, A. Muto, D. Vashaee, X. Chen, J. Liu, M.S. Dresselhaus, G. Chen, Z. Ren, Sci. 320 (2008) 634-638.

[20] F. Delorme, R. Dujardin, F. Schoenstein, B. Pintault, P. Belleville, C. Autret, I. Monot-Laffez, F. Giovannelli, Ceram. Int. 45 (2019) 8313-8318.

[21] G. Tan, L. Zhao, M. Kanatzidis, Chem. Rev. 116 (2016) 12123-12149.

[22] F. Delorme , P. Diaz-Chao, E. Guilmeau, F. Giovannelli, Ceram. Int. 41 (2015) 10038-10043.

[23] F. Giovannelli, C. Chen, P. Diaz-Chao, E. Guilmeau, F. Delorme, J. Eur. Ceram. Soc. 38 (2018) 5015-5020.

[24] C. Chen, F. Giovannelli, J.R. Duclere, F. Delorme, J. Eur. Ceram. Soc. 37 (2017) 4681-4685.

[25] D. Alvarez-Ruiz, F. Azough, D. Hernandez-Maldonado, D.M. Kepaptsoglou, Q.M. Ramasse, S.J. Day, P. Svec, P.Sr Svec, R. Freer, J. Alloys Compd. 762 (2018) 892-900.

[26] A. Giri, J.L. Braun, C.M. Rost, P.E. Hopkins, Scr. Mater. 138 (2017) 134-138.

[27] E.B. Isaacs, G.M. Lu, C. Wolverton, J. Phys. Chem. Lett. 11 (2020) 5577–5583.

[28] A.van Roekeghem, J.Carrete, C. Oses, S. Curtarolo, N. Mingo, Phys. Rev. X 6 (2016) 041061.

[29] F. Gucci, T.G. Saunders, M.J. Reece, Scr. Mater. 157 (2018) 58-61.

[30] J. Yan, F. Liu, G. Ma, B. Gong, J. Zhu, X. Wang, W. Ao, C. Zhang, Y. Li, J. Li, Scr. Mater. 157 (2018) 129-134.

[31] B.R. Ortiz, W. Peng, L.C. Gomes, P. Gorai, T. Zhu, D.M. Smiadak, G. J. Snyder, V. Stevanovic, E. Ertekin, A. Zevalkink, E.S. Toberer, Chem. Mater. 30 (2018) 3395-3409.

[32] Y. Liu, D. Jia, Y. Zhou, Y. Zhou, J. Zhao, Q. Li, B. Liu, J. of Materiomics. 6 (2020) 702-711.

[33] A. V. Kovalevsky, A. A. Yaremchenko, S. Populoh, A. Weidenkaff, J. R. Frade, J. Phys. Chem. C. 118 (2014) 4596-4606.

[34] F. Delorme, C. Chen, F. Schoenstein, N. Jaber, F. Jean, M. Bah, Q. Simon, T. Chartier, P. Laffez, I. Monot-Laffez, F. Giovannelli, Thermochim. Acta. 695 (2021) 178807.

[35] L.H. Brixner, A.W. Sleight, M.S. Licis, J. Solid State Chem. 5 (1972) 247-249.

[36] E-C. Xiao, J. Li, J. Wang, C. Xing, M. Guo, H. Qiao, Q. Wang, Z-M. Qi, G. Dou, F. Shi, J. Materiomics. 4 (2018) 383-389.

[37] W. Jeitschko, Acta cryst. B29 (1973) 2074-2081.

[38] Z. Singh, S.Dash, R.Prasad, V. Venugopal, J. Alloys Compd. 279 (1998) 287-294.

[39] R. Saha, R. Bahu, K. Nagarajan, C.K. Mathews, J. Nucl. Mater. 167 (1989) 271-277.

[40] O. Kubaschewsi, C.B. Alcock, P.J. Spencer. Materials Thermochemistry 6th ed, Pergamon, New York 1993.

[41] A.W. Sleight, L.H. Brixner, J. Solid State Chem. 7 (1973) 172-174.

[42] J.S.O. Evans, T.A. Mary, Int. J. Inorg. Mater. 2 (2000) 143-151.

[43] T. Vargra, J. M Moats, S. V Ushakov, A. Navrotsky, J. Mater. Res. 22 (2007) 2512-2521.

[44] S. Sumithra, A.M. Umarji, Solid State Sci. 8 (2006) 1453-1458.

[45] E. Alleno, D. Bérardan, C. Byl, C. Candolfi, R. Daou, R. Decourt, E. Guilmeau, S. Hébert, J. Hejtmanek, B. Lenoir, P. Masschelein, V. Ohorodnichuk, M. Pollet, S. Populoh, D. Ravot, O. Rouleau, M. Soulier, Rev. Sci. Instrum. 86 (2015) 011301.

[46] J.F. Schatz, G. Simmons, J. Geophys. Res. 77 (1972) 6966-6983.

[47] K.W. Schlichting, N.P. Padture, P.G. Klemens, J. Mater. Sci. 36 (2001) 3003-3010.